AIP Applied Physics Letters

Thermodynamic theory of stress distribution in epitaxial Pb(Zr,Ti)O 3 thin films

H. Joon Kim, S. Hoon Oh, and Hyun M. Jang

Citation: Applied Physics Letters **75**, 3195 (1999); doi: 10.1063/1.125275
View online: http://dx.doi.org/10.1063/1.125275
View Table of Contents: http://scitation.aip.org/content/aip/journal/apl/75/20?ver=pdfcov
Published by the AIP Publishing

Articles you may be interested in
Influence of thermal stresses on the electrocaloric properties of ferroelectric films
Appl. Phys. Lett. **98**, 132907 (2011); 10.1063/1.3573788

Lattice strain in epitaxial Ba Ti O 3 thin films
Appl. Phys. Lett. **88**, 152908 (2006); 10.1063/1.2194231

Effect of anisotropic in-plane strains on phase states and dielectric properties of epitaxial ferroelectric thin films
Appl. Phys. Lett. **86**, 052903 (2005); 10.1063/1.1855389

Domain structure of epitaxial PbTiO 3 thin films on Pt(001)/MgO(001) substrates
J. Appl. Phys. **95**, 236 (2004); 10.1063/1.1631731

Reciprocal space mapping of phase transformation in epitaxial PbTiO 3 thin films using synchrotron x-ray diffraction
J. Appl. Phys. **85**, 1995 (1999); 10.1063/1.369195

This article is copyrighted as indicated in the article. Reuse of AIP content is subject to the terms at: http://scitation.aip.org/termsconditions. Downloaded to IP: 141.223.173.110 On: Mon, 13 Apr 2015 08:30:02

Thermodynamic theory of stress distribution in epitaxial $Pb(Zr,Ti)O_3$ thin films

H. Joon Kim, S. Hoon Oh, and Hyun M. Jang[a)]
Department of Materials Science and Engineering, and National Research Laboratory (NRL) for Ferroelectric Phase Transitions, Pohang University of Science and Technology (POSTECH), Pohang 790-784, Korea

(Received 30 July 1999; accepted for publication 23 September 1999)

A phenomenological thermodynamic model has been developed to account for the effects of the film thickness on various properties of ferroelectric thin films. To this end, we have suitably incorporated a position-dependent stress distribution function into the elastic Gibbs function. Various physical properties can be predicted as a function of the film thickness using this modified thermodynamic formalism. A comparison of the theoretical predictions with experimental values of the average strain and the para-ferro transition temperature indicates that the tensile stress caused by the cubic-tetragonal displacive phase transition dominates over the compressive thermal stress in the epitaxially oriented tetragonal $Pb(Zr,Ti)O_3$ thin films. © *1999 American Institute of Physics.*
[S0003-6951(99)05546-1]

It is known that structure and dielectric/ferroelectric properties of ferroelectric thin films are greatly influenced by the film thickness.[1–4] This thickness dependence is more pronounced in epitaxially grown thin films. Funakubo and co-workers[3] experimentally demonstrated that the lattice parameters and dielectric susceptibilities of epitaxially grown $PbTiO_3$ thin films were increasingly dependent on the film thickness with decreasing total thickness.

Yano and co-workers[4] examined dielectric properties of epitaxially grown $BaTiO_3[100]\|Pt[100]\|MgO[100]$ thin films having various thicknesses. Using phenomenological thermodynamic approach, they further showed that the thickness dependence of dielectric properties was mainly caused by a two-dimensional stress originated from the stress at the film/substrate interface. However, they assumed that a thin film having a certain thickness has its own characteristic value of average stress. Moreover, they simplified the stress distribution over the thickness direction by an average two-dimensional stress, which is valid for an infinitesimally thin film. In reality, however, the stress originated from the interface gradually relaxes with the distance from the interface.

In view of this, the main purpose of the present study is to develop a quantitative thermodynamic model that can account for the effects of the film thickness on various properties of epitaxial thin films. To this end, we have suitably incorporated a position-dependent stress distribution function into the elastic Gibbs function. The thin-film system that we have chosen is an epitaxially grown tetragonal $Pb(Zr,Ti)O_3$ (PZT) because it is the most promising candidate for modern ferroelectric random access memory (FRAM) devices and for numerous thin-film microsensors/actuators used in microelectromechanical system (MEMS) devices.

Considering a thin film having a certain thickness as a piling-up of infinitesimally thin hypothetical two-dimensional layers, one can reasonably assume that the rate of stress relaxation over the thickness direction is proportional to the local stress at this particular position. Then, the variation of a stress over the thickness direction in a given thin film can be represented by the following first-order differential equation:

$$\frac{d\sigma(z)}{dz} = -\alpha_t \sigma(z), \tag{1}$$

where $\sigma(z)$ is the local stress at a position z from the film/substrate interface, and α_t is a decline parameter and is a measure of stress relaxation with the distance. Then, the stress distribution function, $\sigma(z)$, comes out to be

$$\sigma(z) = \sigma_0 e^{-\alpha_t z}, \tag{2}$$

where σ_0 is the stress at the film/substrate interface and is independent of the film thickness.

We will develop a modified phenomenological thermodynamic formalism to determine the two unknown parameters, σ_0 and α_t, from measured values of average strains and average para-ferro transition temperatures for PZT thin films having various thicknesses. Based on the Landau–Devonshire phenomenological theory, one can expand the elastic Gibbs function for a proper ferroelectric derived from a phase of P_{m3m} symmetry using a Taylor series in powers of polarization and stress,[5,6] namely,

$$\begin{aligned}\Delta G = {} & \alpha_1(P_1^2+P_2^2+P_3^2) + \alpha_{11}(P_1^4+P_2^4+P_3^4) \\ & + \alpha_{12}(P_1^2P_2^2+P_2^2P_3^2+P_3^2P_1^2) + \alpha_{111}(P_1^6+P_2^6+P_3^6) \\ & + \alpha_{112}[P_1^4(P_2^2+P_3^2)+P_2^4(P_3^2+P_1^2)+P_3^4(P_1^2+P_2^2)] \\ & + \alpha_{123}P_1^2P_2^2P_3^2 - 1/2 s_{11}(X_1^2+X_2^2+X_3^2) \\ & - s_{12}(X_1X_2+X_2X_3+X_3X_1) - 1/2 s_{44}(X_4^2+X_5^2+X_6^2) \\ & - Q_{11}(X_1P_1^2+X_2P_2^2+X_3P_3^2) - Q_{12}[X_1(P_2^2+P_3^2) \\ & + X_2(P_3^2+P_1^2) + X_3(P_1^2+P_2^2)] - Q_{44}(X_4P_2P_3 \\ & + X_5P_3P_1 + X_6P_1P_2),\end{aligned} \tag{3}$$

[a)]Electronic mail: hmjang@postech.ac.kr

This article is copyrighted as indicated in the article. Reuse of AIP content is subject to the terms at: http://scitation.aip.org/termsconditions. Downloaded to IP: 141.223.173.110 On: Mon, 13 Apr 2015 08:30:02

where P_i and X_i, respectively, are the magnitude of the polarization vector along the direction, i, and the i-component stress, respectively. In the reduced notation, X_1, X_2, X_3 denote the tensile stresses and X_4, X_5, X_6 the shear components. α_1 is the dielectric stiffness and is assumed to be a linear function of temperature near the Curie temperature (Curie–Weiss law). α_{ij} and α_{ijk} are the high-order stiffness coefficients at a constant stress, s_{ij} are the elastic compliances measured at a constant polarization, and Q_{ij} are the electrostrictive coefficients written in polarization notation. All the coefficients except for α_1 are assumed to be independent of temperature, and their optimized values are given in a series of papers reported by Haun and co-workers.[7,8]

We now introduce the stress distribution function into the elastic Gibbs function for a tetragonal phase. The following relations hold under a two-dimensional stress $\sigma(z)$ at a given position z:

$$X_1=X_2=\sigma(z), \quad X_3=X_4=X_5=X_6=0. \tag{4}$$

The spontaneous polarization ($P_s=P_3$) can be derived from ΔG for a tetragonal phase using the stability criterion, i.e., $\partial\Delta G/\partial P_i=E_i=0$:

$$P_1^2=P_2^2=0,$$

$$P_3^2(z)=P_s^2(z)=\frac{-\alpha_{11}+[\alpha_{11}^2-3\alpha_{111}\{\alpha_1-2Q_{12}\sigma(z)\}]^{1/2}}{3\alpha_{111}}. \tag{5}$$

Similarly, the strain can be derived using the relation, $\partial\Delta G/\partial X_i=-x_i$, and x_1 for a tetragonal phase is given by

$$x_1(z)=\frac{Q_{12}\{-\alpha_{11}+[\alpha_{11}^2-3\alpha_{111}(\alpha_1-2Q_{12}\sigma(z))]^{1/2}\}}{3\alpha_{111}} +(s_{11}+s_{12})\sigma(z). \tag{6}$$

On the other hand, the strain developed along the a axis can be estimated from the experimentally determined lattice parameters using the following relation:

$$x_1=(a_T-a_c')/a_c', \tag{7}$$

where a_T is the a-axis lattice constant for a tetragonal phase, and a_c' is that for a hypothetical cubic phase extrapolated to room temperature.

To correlate the above theoretical prediction with experimentally available values, we have further computed average values of the strain as a function of the film thickness. To do this, we have used the mean value theorem. Using Eq. (6) one can eventually obtain the following expression of $\overline{x_1}$ after a tedious integration procedure:

$$\overline{x_1}=\frac{1}{t}\int_0^t x_1(z)dz$$

$$=-\frac{Q_{12}\alpha_{11}}{3\alpha_{111}}-\frac{Q_{12}}{3\alpha_{111}\alpha_t t}\left[2\{\sqrt{ae^{-\alpha_t t}+b}-\sqrt{a+b}\} + \sqrt{b}\left\{\ln\left(\frac{\sqrt{ae^{-\alpha_t t}+b}-\sqrt{b}}{\sqrt{ae^{-\alpha_t t}+b}+\sqrt{b}}\right)-\ln\left(\frac{\sqrt{a+b}-\sqrt{b}}{\sqrt{a+b}+\sqrt{b}}\right)\right\}\right] -(s_{11}+s_{12})\frac{\sigma_0}{t\alpha_t}[e^{-\alpha_t t}-1], \tag{8}$$

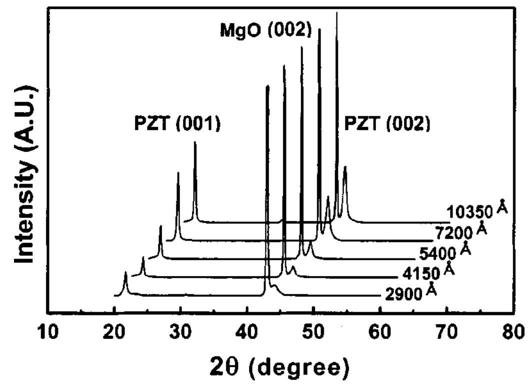

FIG. 1. X-ray θ–2θ scan profiles of $PbZr_{0.4}Ti_{0.6}O_3$ thin films with various thicknesses.

where $a=6\alpha_{111}Q_{12}\sigma_0$ and $b=\alpha_{11}^2-3\alpha_{111}\alpha_1$.

We now consider the para-ferro transition temperature (T_c) as a function of $\sigma(z)$. Using the expression of the elastic Gibbs function at the Curie point and its partial derivative with respect to P_c in the absence of any external field (i.e., $\partial\Delta G/\partial P_c=E_c=0$), one can derive an expression for the spontaneous polarization at the Curie point.[6] Substituting this expression into the stability criterion, $\partial\Delta G/\partial P_c=E_c=0$, and using the mean value theorem again, we have eventually obtained the following relation for the average para-ferro transition temperature in the tetragonal phase field:

$$\overline{T_c}=\frac{1}{t}\int_0^t T_c(z)dz$$

$$=T_0+\frac{\alpha_{11}^2}{4\beta\alpha_{111}}-\frac{2Q_{12}\sigma_0}{\beta\alpha_t t}[e^{-\alpha_t t}-1] +\frac{2(s_{11}+s_{12})\sigma_0^2}{2\beta\alpha_t t}[e^{-2\alpha_t t}-1] +\frac{12\alpha_{111}^4(s_{11}+s_{12})\sigma_0^4}{4\beta\alpha_t t\alpha_{11}^4}[e^{-4\alpha_t t}-1], \tag{9}$$

where T_0 is the Curie–Weiss temperature, $\beta\equiv 1/2\epsilon_0 C$, and C is the Curie constant.

To examine our theoretical treatments, we have prepared epitaxially oriented tetragonal PZT thin films (with Zr/Ti $=0.4/0.6$) having various film thicknesses on MgO(001) using a pulsed laser deposition (PLD) method. The deposition conditions used in the present study are as follows: (i) LASER source; KrF eximer with a pulse width of 30 ns at 10 Hz, (ii) fluence; 60 mJ/cm^2, (iii) oxygen pressure; 0.05 Torr, (iv) substrate temperature; 650 °C.

The c-axis lattice constant was estimated using conventional x-ray θ–2θ scans (with Cu $K\alpha$ radiation) while the a-axis lattice constant was determined using {303} rocking curves. The x-ray diffraction (XRD) θ–2θ patterns of the PZT thin films are shown in Fig. 1. Only peaks originating from the $(00l)$-type diffraction were found. This indicates that the films have a tetragonal perovskite structure and are highly c-axis oriented. Using $2\theta_{(001)}$ values obtained from the θ–2θ scans we have calculated the c-axis lattice parameters. To evaluate the lattice parameters in the direction parallel to the film/substrate interface (i.e., a axis), the asymmetric {303} rocking experiment was performed (see Fig. 2). The

This article is copyrighted as indicated in the article. Reuse of AIP content is subject to the terms at: http://scitation.aip.org/termsconditions. Downloaded to IP: 141.223.173.110 On: Mon, 13 Apr 2015 08:30:02

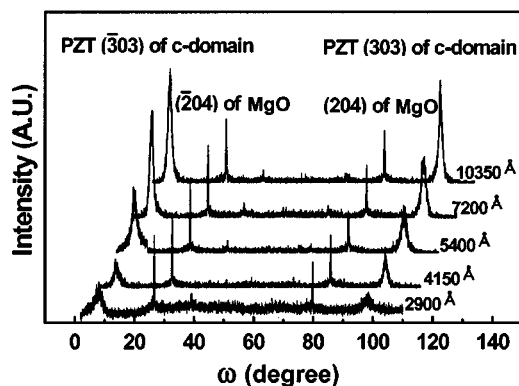

FIG. 2. Asymmetric {303} rocking curves of $PbZr_{0.4}Ti_{0.6}O_3$ thin films with various thicknesses.

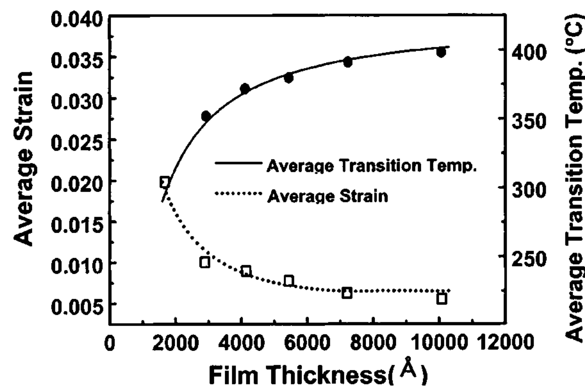

FIG. 3. Comparison of the theoretical predictions with the experimental data of average strain and transition temperature of $PbZr_{0.4}Ti_{0.6}O_3$ thin films as a function of film thickness.

specimen is rotated to obtain the rocking curves of (303) peaks while the reflected beam is collected in a counter fixed at the $2\theta_{(303)}$ corresponding to the Bragg angle for (303) planes. The a-axis lattice parameter is determined using the following relation:

$$a_T = \frac{c}{\tan(\Delta\omega_{303}/2)}, \tag{10}$$

where $\Delta\omega_{303}$ is the difference between ω_{303} for (303) planes and $\omega_{\bar{3}03}$ for ($\bar{3}$03) planes in the rocking curves. One can readily obtain the average strain values ($\overline{x_1}$) of epitaxial $PbZr_{0.4}Ti_{0.6}O_3$ thin films at room temperature using these experimental results and Eq. (7).

The average para-ferro transition temperatures of epitaxial $PbZr_{0.4}Ti_{0.6}O_3$ thin films with various thicknesses were measured using a differential thermal analyzer (DTA7, Perkin Elmer). The film thickness was measured using an α stepper (Tencor Instruments).

We are now in a position to estimate the two unknown parameters, σ_0 and α_t in Eq. (2). For temperatures above T_c, σ_0 has only a thermal stress. Thus, we can directly obtain σ_0 for $T > T_c$ from the difference in the thermal expansion coefficient between PZT and MgO substrate. Using these values of σ_0 and the experimental values of the average transition temperature, one can numerically estimate α_t as a function of the film thickness from Eq. (9). We found that α_t was essentially independent of temperature with a good linear correlation between α_t and the film thickness, t. The next step is to estimate σ_0 for $T < T_c$. Using the estimated value of α_t and the experimental value of the average strain for a given film thickness, one can subsequently estimate σ_0 for room temperature from Eq. (8). Consequently, we have obtained the following stress distribution function for the epitaxially oriented tetragonal PZT thin films:

$$\sigma(z,t) = \sigma_0 e^{-\alpha_t z}, \tag{11}$$

where $\sigma_0 = +1.16\,\mathrm{GPa}$ at room temperature, and $\alpha_t = +3.925\times10^{-4} - 2.325\times10^{-8}t$ in an Å unit. A positive sign of σ_0 signifies a tensile stress at the interface. α_t is independent of temperature and has a dimension of $(\mathrm{length})^{-1}$.

Figure 3 compares the theoretical computations of the average strain and the transition temperature with experimental values as a function of the film thickness, t. As shown in the figure, the theoretical prediction reasonably describes the experimental values for a wide range of the film thickness. One important feature of Fig. 3 is that the average strain of the PZT thin film decreases while the average transition temperature increases rapidly with increasing film thickness. This indicates that the thin film is under a high tensile stress. Our theoretical computation clearly predicts a reverse trend under a compressive stress. This further indicates that, for epitaxially grown tetragonal PZT thin films, the tensile stress caused by the cubic-tetragonal displacive phase transition (GPa order) dominates over the compressive thermal stress (MPa order).

In conclusion, a phenomenological thermodynamic model has been developed to account for the effects of the film thickness on various properties of epitaxial ferroelectric thin films. By correlating the present theoretical predictions with the experimental data, it is shown that the tensile stress caused by the cubic-tetragonal displacive phase transition dominates over the compressive thermal stress in the epitaxially grown tetragonal PZT thin films on MgO(001) substrates.

This work was supported by the Korea Institute of Science and Technology Evaluation and Planning (KISTEP) through the NRL project and by POSTECH through ''POSTECH/BSRI Special Fund-1999.''

[1] F. Tsai and J. M. Cowley, Appl. Phys. Lett. **65**, 1906 (1994).
[2] Y. G. Wang, W. L. Zhang, and P. L. Zhang, Phys. Rev. B **51**, 5311 (1995).
[3] H. Funakubo, T. Hioki, M. Otsu, K. Shinozaki, and N. Mizutani, Jpn. J. Appl. Phys., Part 1 **32**, 4175 (1993).
[4] Y. Yano, K. Iijima, Y. Daltoh, T. Terashima, and Y. Bando, J. Appl. Phys. **76**, 7833 (1994).
[5] A. Amin, R. E. Newnham, and L. E. Cross, Phys. Rev. B **34**, 1595 (1986).
[6] S. H. Oh and H. M. Jang, Appl. Phys. Lett. **72**, 1457 (1998).
[7] M. J. Haun, E. Furman, S. J. Jang, H. A. McKinstry, Z. Q. Zhuang, T. R. Halemane, and L. E. Cross, Ferroelectrics **99**, 13 Parts I, II, III, IV, and V (1989).
[8] M. J. Haun, Z. Q. Zhuang, E. Furman, S. J. Jang, and L. E. Cross, J. Am. Ceram. Soc. **72**, 1140 (1989).

This article is copyrighted as indicated in the article. Reuse of AIP content is subject to the terms at: http://scitation.aip.org/termsconditions. Downloaded to IP: 141.223.173.110 On: Mon, 13 Apr 2015 08:30:02